Journal of Ceramic Processing Research. Vol. 26, No. 1, pp. 177~191 (2025)
(Received 5 August 2024, Received in revised form 11 October 2024, Accepted 15 October 2024)
https://doi.org/10.36410/jcpr.2025.26.1.177

J O U R N A L O F
Ceramic Processing Research

Advances in synthesis, characterization and theories of high-temperature superconducting materials

Zihao Wu*
Department of Physics, Capital Normal University, Beijing 100080, China

High-temperature superconducting materials play an important role in industry, significantly improving the efficiency of power transmission and reducing energy consumption, and can bring major technological breakthroughs in areas such as nuclear fusion, energy storage, and magnetic levitation, which opens the new area in superconducting science and material science. High current carrying capacity as well as excellent magnetic and thermal properties can make high-temperature superconductors have wide application potential in energy transmission, medical imaging, magnetic suspension, and other fields. However, the study of high-temperature superconductors remains challenging. Understanding the superconducting mechanism, raising the critical temperature, and preparing complex structure are the main focuses of current researches. This paper briefly outlines the development of high-temperature superconductivity research. It begins with an exploration of BCS theory, which is closely related material thermodynamic properties. It then looks into the theory of electron interaction and discusses the idea of magnetic vortices. The focus is on key materials like cuprates and iron pnictides, highlighting their growing use in technology, aiming to enhance understanding of this field.

Keywords: High-temperature superconductivity, Superconductivity theory, Superconductivity research focus, Superconductivity materials.

Introduction

Resistance is a fundamental physical quantity used to describe the degree of hindrance to the flow of electric current in an object. In Ohm's law, resistance is defined as the ratio of voltage to current, measured in ohms [1, 2]. The magnitude of resistance depends on factors such as the properties of the material, the shape and size of the object, and temperature. At a certain temperature, for a given material, resistance is directly proportional to the length of the object and inversely proportional to its cross-sectional area, a relationship known as the law of resistivity [3-5]. Ideal resistors only exhibit resistance without capacitance and inductance, hence current and voltage are in phase. Some materials, below a specific critical temperature, can conduct current without loss, demonstrating a state of zero resistance, a phenomenon known as superconductivity [6]. Materials exhibiting superconductivity when temperatures exceed 77K (the boiling point of liquid nitrogen) are termed high-temperature superconducting materials. The phenomenon of superconductivity was first observed in 1911 by the Dutch physicist H. K. Onnes during experiments. The theoretical explanation of superconductivity has been a significant subject in physics. In 1957, J. Bardeen, L. N. Cooper, and J. R. Schrieffer proposed the famous BCS theory, explaining conventional low-temperature superconductivity, with these superconductors referred to as type I superconductors. The BCS theory is based on the concept of Cooper pairs, where at low temperatures, two electrons can form a paired state, allowing them to move throughout the crystal lattice without resistance. However, the BCS theory cannot explain all superconducting phenomena. In 1986, the discovery of high-temperature superconductors contradicted the predictions of the BCS theory, leading to the classification of these superconductors as type II superconductors. High-temperature superconducting materials mainly include Bi-based superconductors (BSCCO), Y-based superconductors (YBCO), iron-based superconductors, MgB_2, etc [7-9]. The critical temperature of high-temperature superconductors is much higher than the range predicted by the BCS theory, and the mechanism of superconductivity in these materials remains an important unresolved issue in physics. Superconductivity plays a crucial role in various applications, including maglev trains, particle accelerators, medical imaging devices, etc. However, the application of superconducting materials is still limited due to their typically low critical temperatures. Discovering or manufacturing materials exhibiting superconducting properties at room temperature would trigger a technological revolution [10].

Recently, high-temperature superconducting materials

*Corresponding author:
Tel : +86 13693669780
E-mail: zihaowuzh@outlook.com

have been widely applied in scientific research, electricity, medicine, transportation, and other fields. In terms of electricity, we can greatly reduce the energy loss in the transmission process by using superconducting materials in transmission lines to transmit electricity over long distances. For example, REBaCuO (RE123) high-temperature superconducting coating conductor, which produced by thin film epitaxy and biaxial texture technology on flexible metal baseband, solves the problems of difficult machining and weak grain boundary connection of ceramic copper oxygen high-temperature superconductor [11]. The key technology of such a high-temperature superconducting coating conductor is the construction of its superconducting strips [12], whose outermost layer is a protective layer composed of metal silver or metal copper; The second layer is a superconducting layer made of RE123 high-temperature superconducting material; The third layer is a buffer layer with biaxial texture, stable chemical properties and no reflection with RE123 material. The innermost is the flexible metal substrate, and it is worth mentioning that chemical reactions cannot occur between the buffer layer and the flexible metal substrate.

In the medical field, the application of high-temperature superconducting materials in clinical medical research is also unlimited. Superconducting materials made of superconducting coils can generate a strong and constant magnetic field. This superconducting magnet is exactly what is needed for high-resolution MRI in clinical medicine. Compared with ordinary magnets, superconducting magnets have less energy consumption, higher stability, and smaller size.

In transportation, high-temperature superconducting materials can also play a crucial part in superconducting magnetic levitation. Due to the Meissner effect, when the superconductor was placed in an ordinary magnetic field, the magnetic field lines cannot pass through the superconductor but are tightly surrounded around the superconductor. Due to the action of these magnetic field lines, the superconductor is bound in these magnetic field lines, achieving the effect of suspension. Compared with ordinary maglev technology, superconducting maglev technology will show more stable, high speed, and safety characteristics.

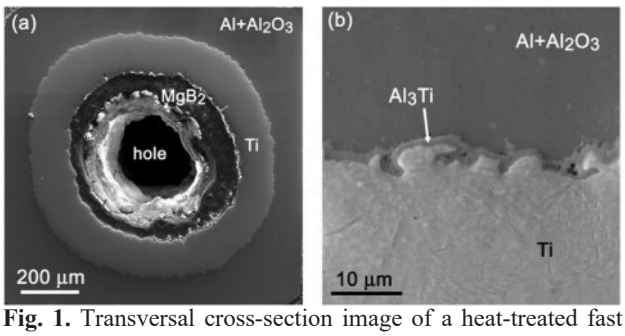

Fig. 1. Transversal cross-section image of a heat-treated fast ramp heat treat-ments (~25 °C/min) with the setting temperature 628-635 °C and overshoot up to 640-646.5 °C were appliedfor deformed B HITEMAL wires (a) and a detail of an Al_3Ti reaction layer at the Ti/Al interface of the wire (b) [13].

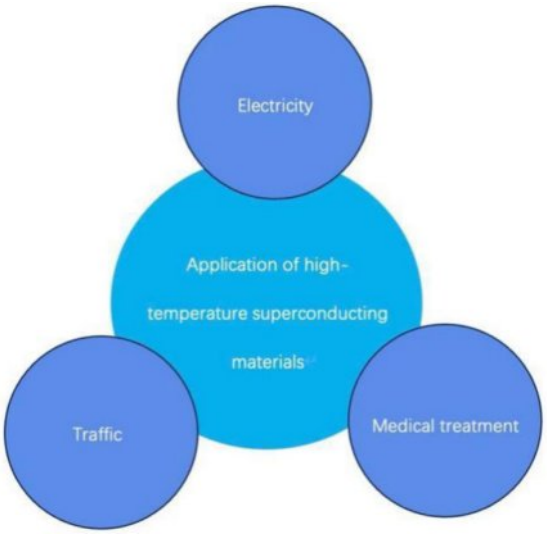

Fig. 2. Application of high-temperature superconducting materials [14].

Theory

BCS theory

As early as 1911, the Dutch physicist H. K. Onnes found the phenomenon of superconductivity by reducing the temperature of metal mercury to 4.2K, that is, the phenomenon that the resistance of metal mercury suddenly drops to 0 at a certain critical temperature. But it wasn't until 1957 that the microscopic mechanism was explained. J. Bardeen, L.N. Cooper, and J.R. Schrieffer, and proposed the famous BCS theory based on the near-free electron model and the premise of very weak electron-phonon coupling [15], they were thus awarded the Nobel Prize in Physics [16]. The mechanism of BCS theory is as follows: When atoms are arranged in a crystal, it is called the spatial lattice of their arrangement law a lattice. In solids, lattice vibrations arise due to the periodic arrangement of atoms or ions in the crystal structure, which undergo tiny oscillations about their equilibrium positions. An increase in temperature leads to enhanced thermal vibrations of the atoms and ions within the crystal, thereby increasing the overall energy of the lattice. These thermal vibrations are a result of the mutual interactions between the atoms or ions in the crystal, with their energy levels and frequencies being influenced by the temperature. The generation of lattice vibrations can be explained through the phonon theory, where phonons are the fundamental quanta of lattice vibrations in a crystal, akin to particles in quantum mechanics; lattice vibrations can thus be viewed as the propagation of phonons through the lattice, with their frequencies and wave vectors characterizing the vibrational modes. As the temperature increases, the thermal vibrations

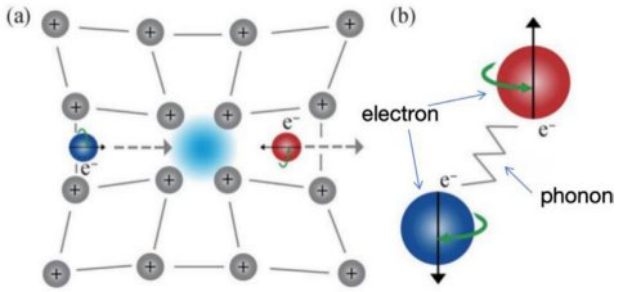

Fig. 3. Schematic diagram of BCS theory [17].

within the crystal become more vigorous, and the energy of the phonons also rises, leading to changes in their frequencies. These thermally excited vibrations impact the lattice's structure and properties, causing alterations in thermodynamic properties such as the coefficient of thermal expansion and specific heat capacity of the crystal. Therefore, temperature emerges as a critical factor influencing both the lattice properties and the intensity of vibrations. Lattice vibrations indirectly create a mutual attraction between electrons with opposite spin and momentum near the Fermi surface, and they paired together to form a "Cooper pair". Only when the Cooper pair is formed, the energy of the system is lowest, and the Cooper pair can move in the lattice without loss, showing no resistance phenomenon. Thus, the metal exhibits superconducting properties. The BCS theory was the first to reveal the microscopic mechanism of superconductivity and explain and predict other properties of superconductors.

Obviously, the mechanism of high-temperature superconductivity is closely intertwined with thermodynamics. Although the specific mechanism remains to be fully elucidated, thermodynamic theory provides a crucial framework and perspective for explaining this physical phenomenon.Thermodynamics, which explores the characteristics and laws of thermal motion of matter from a macroscopic perspective, offers a solid theoretical foundation for the study of high-temperature superconductivity. High-temperature superconductivity involves the pairing and transport of electrons within materials, a process accompanied by the conversion and transfer of energy.The interaction between electrons, including their pairing and transport, is crucial to the formation of the high-temperature superconducting state. Principles such as Coulomb's law and statistical mechanics in thermodynamic theory can describe the interactions and energy states of electrons, thereby revealing the essence of high-temperature superconductivity. Although the BCS theory primarily explains low-temperature superconductivity, the electron pairing mechanism it reveals still provides valuable insights for the study of high-temperature superconductivity.

However, when the critical temperature of superconductors exceeds the range predicted by the BCS theory, it fails to provide a satisfactory explanation. This is what we call high-temperature superconductors or type II superconductors. The critical temperatures of these materials can reach the boiling point of liquid nitrogen (77 K) or even higher, far exceeding the upper limit predicted by the BCS theory based on the mechanism of Cooper pair formation mediated by phonons (approximately 30 K). In an attempt to explain the mechanism of high-temperature superconductivity, theories such as strong correlation electron theory and spin-fluctuation theory have emerged.

Strong Correlation Electron Theory

Strong correlation electron systems are an important concept in condensed matter physics, describing material systems where electron interactions are strong enough to alter their fundamental properties. In such systems, electron interactions cannot be neglected, and the system cannot be simply viewed as a collection of independent electrons. This contrasts with weakly correlated electron systems, where properties can be understood through the behavior of individual electrons.

The theory of strongly correlated electrons, as a theoretical framework for delving into the behavior of electrons in complex systems, aims to reveal the dynamic characteristics of electrons under strong interactions and their intrinsic connections with the overall properties of the system. In strongly correlated electron systems, the interactions between electrons are particularly significant, making it impossible to simply treat the system as a collection of independent electrons. Instead, the profound influence of electron-electron interactions on the overall properties of the system must be fully considered. With the increase in temperature, the behavior of electrons in strongly correlated electron systems undergoes a series of complex and subtle transformations. These transformations may include phase transitions from ordered phases to disordered phases. This transition is not merely a simple change of state but involves profound changes in the electronic structure and the overall properties of the system. During the phase transition, significant changes may occur in the arrangement, motion state, and interactions of electrons, leading to notable alterations in the overall properties of the system. Changes in these physical properties, such as electrical conductivity, thermal conductivity, and specific heat capacity, are direct reflections of changes in electron behavior. For instance, electrical conductivity, as a crucial physical quantity measuring the ability of electrons to transport within a material, provides insights into the transport behavior of electrons in the system. As temperature rises, scattering between electrons intensifies, increasing the hindrance to electron transport, i.e., enhancing the damping effect. This damping effect makes it more difficult for electrons to move within the system, thereby affecting their conductive behavior and resulting in a decrease in electrical conductivity. Similarly, changes in thermal conductivity and specific

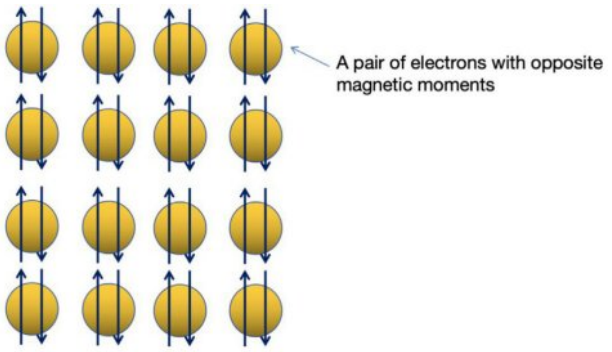

Fig. 4. Schematic of a strongly correlated electronic system.

heat capacity are also closely related to electron behavior. Thermal conductivity reflects the ability of a material to conduct heat, while specific heat capacity describes the change in temperature when a material absorbs or releases heat. In strongly correlated electron systems, these property changes reflect the interactions between electrons and the influence of temperature on electron behavior. Notably, there is a close relationship between electron correlation effects and high-temperature superconductivity. High-temperature superconductivity remains a significant challenge in modern physics, with its underlying mechanisms yet to be fully elucidated. However, increasing research indicates that electron correlation effects play a crucial role in high-temperature superconductivity. Through in-depth studies of electron behavior in strongly correlated electron systems, we can provide new perspectives and approaches for understanding high-temperature superconductivity. In summary, the theory of strongly correlated electrons, by delving into the behavior of electrons in complex systems, provides a powerful theoretical tool for understanding complex physical phenomena such as high-temperature superconductivity. With further research, we hope to unveil the mysteries behind complex physical phenomena like high-temperature superconductivity and contribute significantly to the advancement of physics.

In the field of high-temperature superconductivity research, the theory of strongly correlated electrons plays a pivotal role, offering crucial theoretical support for our understanding of this complex phenomenon. The emergence of this theoretical framework has not only enriched our knowledge of superconductivity but also provided powerful guidance for subsequent experimental investigations and theoretical explorations. As for high-temperature superconductors, the interactions between electrons are particularly intense. This strong correlation effect renders traditional superconductivity theories inapplicable to a certain extent. Taking copper oxide high-temperature superconductors as an example, the significant electron correlation effects render the phonon-mediated Cooper pair formation mechanism in BCS theory inapplicable in these materials. Consequently, there is a need to seek new theoretical frameworks to explain the superconductivity mechanisms in these high-temperature superconductors. The theory of strongly correlated electrons emerged to provide a fresh perspective for explaining the superconductivity mechanisms in high-temperature superconductors. This theory posits that the strong correlation effects among electrons are the crucial factor driving superconductivity in these materials. Such strong correlation effects may stem from direct interactions between electrons or indirect interactions mediated by certain mechanisms (such as spin fluctuations). These interactions lead to the formation of a special pairing state among electrons, known as superconducting pairing. It is noteworthy that the theory of strongly correlated electrons is not a single theoretical model but an umbrella term encompassing a range of related theories. These theories adopt different methods and assumptions in describing the strong correlation effects among electrons, but their common denominator is the emphasis on the significance of electron-electron interactions. While these theories offer a potential explanatory framework, the specific superconductivity mechanisms remain an unresolved issue. Therefore, further in-depth investigations into the theory of strongly correlated electrons are necessary, coupled with experimental data to validate and refine

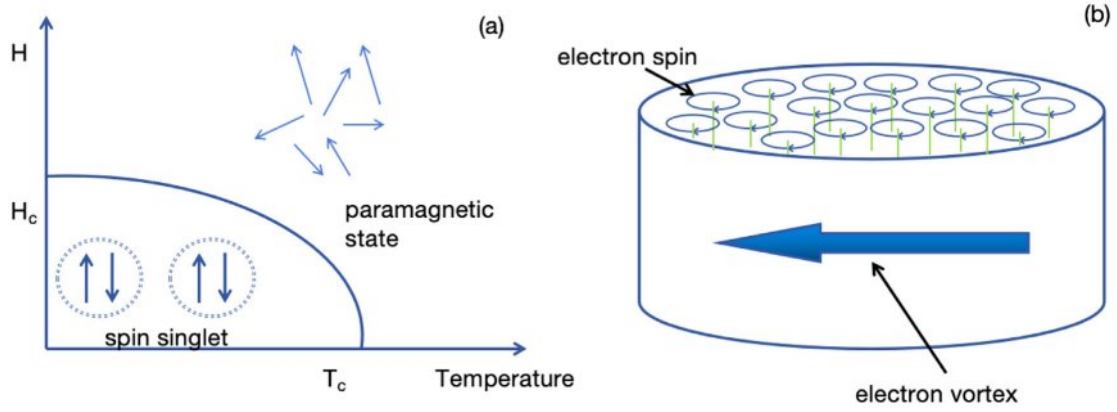

Fig. 5. (a) Conventional superconductors from the perspective of spin orientation, (b) type II the mixed state of superconductors.

these theories. Through continued exploration and innovation, we hope to unveil the mysteries surrounding high-temperature superconductivity.

Spin-Fluctuation Theory

The Spin-Fluctuation Theory is a theoretical framework aimed at explaining high-temperature superconductivity phenomena. Its primary premise is that superconducting pairing in high-temperature superconductors is induced by fluctuations (or waves) in electron spins, rather than by phonon-mediated Cooper pairs as posited in the BCS theory.

The theory of spin fluctuations serves as an important theoretical framework for exploring superconductivity, providing a unique perspective for understanding the behavior of electrons in the lattice and the formation of the superconducting state. According to this theory, electron spins within the lattice can form vortex-like structures, and the intensity of these spin vortices exhibits a close correlation with the system's temperature. Within the theoretical framework of statistical physics, the principle of thermal equilibrium reveals the inherent connection between temperature and entropy [18]. As the temperature of a system rises, its internal entropy also increases accordingly. In spin systems, this entropy increase manifests as a significant enhancement of spin fluctuations. Specifically, as the temperature increases, the flipping frequency of electron spins rises, promoting the formation and enhancement of spin vortices. These spin vortices not only increase in number but also in intensity, becoming a crucial factor influencing superconductivity.

Furthermore, according to the second law of thermodynamics, namely the principle of entropy increase, the evolution of spin vortices is accompanied by an increase in system entropy. This principle further emphasizes the central role of spin fluctuations in high-temperature superconductivity. Importantly, under specific conditions, spin vortices can induce electrons to enter a paired state, thereby triggering superconductivity. This mechanism differs fundamentally from the Cooper pair formation mechanism in BCS theory. In BCS theory, electron pairing occurs through phonon exchange, while the theory of spin fluctuations highlights the direct inducing role of electron spin fluctuations in superconducting pairing. Notably, the theory of spin fluctuations also predicts that superconducting pairs in high-temperature superconductors should exhibit specific momentum distributions, governed by the characteristics of spin fluctuations. To verify this prediction, researchers have conducted numerous rigorous experimental studies. The results of these studies not only support the validity of the spin fluctuation theory but also provide valuable insights for a deeper understanding of high-temperature superconductivity. Moreover, spin fluctuations play a crucial role in defining the superconducting properties of materials. Studies have shown that superconducting materials with higher critical temperatures (Tc) often exhibit higher symmetry, with cubic structures often associated with higher Tc values. This finding further underscores the importance of spin fluctuations in superconductivity and provides useful insights for exploring novel high-temperature superconducting materials [20].

In conclusion, the theory of spin fluctuations, with its unique perspective and profound insights, offers a new avenue for understanding high-temperature superconductivity. This theory not only reveals the close relationship between spin vortices and temperature but also clarifies the mechanism of spin vortex-induced superconducting pairing. With further research, the study of spin fluctuations injects new vitality into the development of related fields and drives the scientific community to further explore and understand superconductivity.

Synthesis and Characterization of Superconducting Materials

In order to synthesize and characterize the material properties of superconducting materials, several very important research methods and means will be used. X-ray Diffraction (XRD) can be used to determine the crystal structure, crystal size, crystal orientation, crystal defect and other information of a sample by measuring the Angle and intensity of X-ray diffraction in the sample. Transmission electron microscopy (TEM) can provide atomic-level images to observe the microstructure of materials, crystal defects, and the shape and size distribution of nanoparticles. Powder-in Tube (PIT) enables continuous production of materials and is suitable for the preparation of materials in the shape of strips or films. The Physical Property Measurement System (PPMS) can be measured under different temperature and magnetic field conditions and is often used to check the physical properties of materials to verify the functionality of materials. The structure and properties of the materials prepared by PIT were obtained by XRD, TEM and PPMS.

X-ray diffraction

X-ray Diffraction (XRD) is of an important means to study the structure of high-temperature superconducting materials. The XRD instrument has three main parts (as shown in Fig. 6): first, the X-ray tube, which emits highly stable, and can control the change of wavelength of X-rays; The second is the ray detector, which can receive and detect the X-ray after the diffraction, and put it into the computer to process the map; Finally, the processing and analysis system of the diffraction pattern in computer.

The XRD instrument works as follows: Place the sample in the middle of the sample table of the XRD instrument and hit the X-ray onto the sample. X-rays are high-energy rays, and each repeat period is a wavelength λ, about 0.01 nm-10 nm. This is on the same

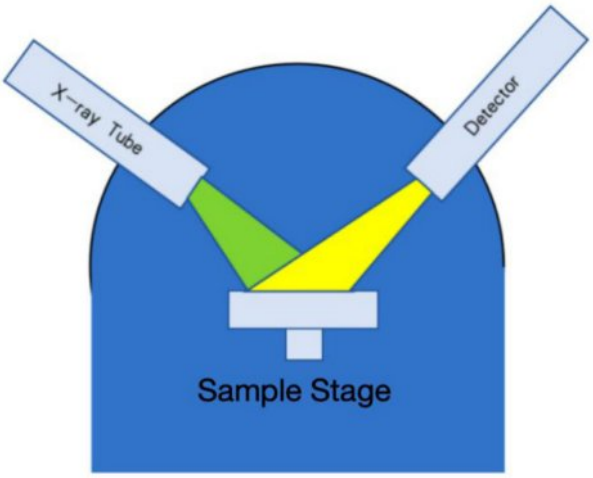

Fig. 6. X-ray diffraction diagram.

order of magnitude as the spacing of atoms or lattices, and diffraction occurs. When the X-rays interact with each other in phase, this signal is "interfered with in phase" and thus amplified. If it is a wave of different phases, "destructive interference" will occur, and the signal will disappear. After that, the X-ray tube and the ray detector run in sync to ensure acceptance. The materials detected by XRD are generally composed of small crystal structures, mostly solid blocks of single crystals, powders, polycrystals, or microcrystals. Each crystal consists of a regular arrangement of atoms, and each atom consists of a nucleus and a cloud of electrons around it. When X-rays hit an atom, "elastic scattering" occurs, that is, the energy is absorbed by electrons outside the nucleus, but the energy of the X-rays is not enough to stimulate the electrons to escape, so the absorbed energy is emitted as a new form of X-ray, and its energy remains the same as before absorption. In the crystal structure, the atomic arrangement is repeated, forming different crystal faces, which are separated by different distances from each other. When X-rays hit a regularly arranged atomic plane, scattering occurs. Only at a special Angle can the scattered signal be greatly amplified. The scattered X-rays will have coherent interference, resulting in the diffraction phenomenon. However, coherent interference also has its condition, that is, the wavelength of the scattered X-rays must be in phase, so the scattered wavelength needs to pass through an integer wavelength. The Angle between the incident light and the scattered light is called 2θ.

As shown in Fig. 6, X-rays are produced by high-speed electrons hitting a metal target. When an electron hits a metal target, it knocks out the electrons inside the target atom, causing a change in the energy level of the electrons inside the atom, resulting in X-rays. When X-rays are irradiated into the crystal, the atoms in the crystal will scatter the X-rays, because the atoms in the crystal are arranged regularly, so the scattered X-rays also have a certain law, which forms the diffraction phenomenon. X-ray diffraction through the sample after systematic analysis, will form a peak diagram of the sample's atomic structure. For example, in Fig. 7a, there is the X-ray diffraction image of $LuH_{2\pm x}N_y$, and in Fig. 7b, it shows the physical XRD image. The peak graph can be used for qualitative analysis of materials, calculation of lattice spacing, calculation of particle size, and simple quantitative analysis. When comparing the XRD diffraction pattern, if the peak value shifts to the left, it means that the lattice constant becomes larger, and an atom with a larger radius than the original atom may be doped based on the original atom or a lattice distortion occurs, and vice versa. In the study of superconducting materials, XRD can be used to determine the crystal structure of superconducting materials, including lattice parameters, space groups, atomic positions, etc. This is essential for understanding superconductivity mechanisms and optimizing superconductivity properties. It can also be used to detect various phases in superconducting

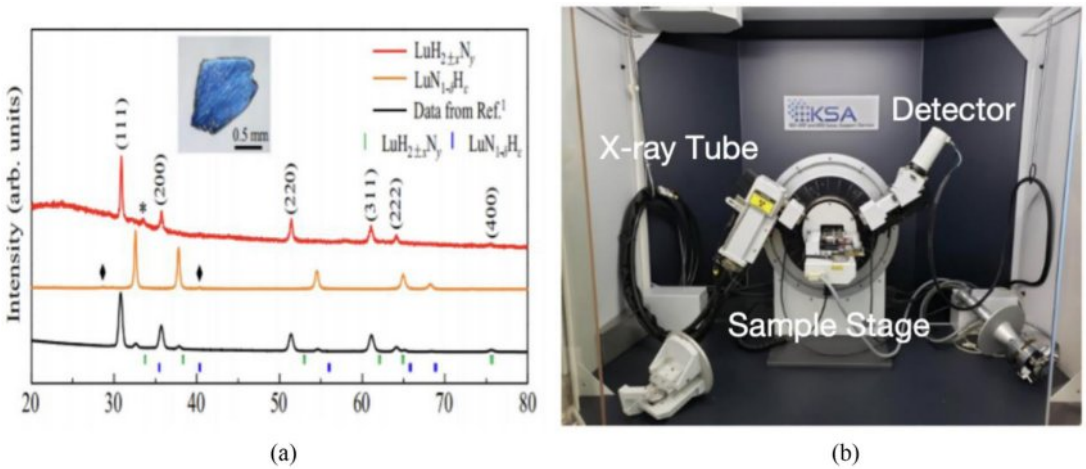

Fig. 7. (a) Typical XRD pattern (red line) of our produced nitrogen doped lutetium hydride sample $LuH_{2\pm x}N_y$ [21], (b) X-ray diffraction [22].

samples, including both superconducting and non-superconducting phases. This is important for controlling the phase composition of the sample and optimizing its superconducting properties. By analyzing XRD patterns, information about the internal strains and defects of superconducting materials can be obtained. These factors may affect superconductivity.

Transmission Electron Microscopy

Transmission electron microscopy (TEM) is also an important instrument for observing and analyzing the structure and properties of superconducting materials. TEM consists of three parts (Fig. 8): an electron gun, an electromagnetic lens, and an electron detector.

TEM works on the principle of wave-particle duality, that is, using the fluctuations of the electron beam in place of natural light. TEM can observe the size and morphology of the material's microscopic morphology, magnifying very thin sample images down to the atomic level.

A transmission mirror is an electron gun that emits an electron beam and transmits electrons through the sample to collect transmitted electron imaging. TEM is to place a thin sample along the vertical direction of the electron beam, the electron beam is accelerated by emission to obtain a certain speed, and is focused on the sample through the lens. After the light beam passes through the sample, the sample acts on it to produce an image. The most commonly used mode of TEM is bright field imaging mode, where the material is thin and more electrons pass through, the image is brighter. Conversely, where the material is thick, fewer electrons are passing through, and the image is relatively dark. The beam is then amplified and detected by other lenses, as if fluorescent.

As shown in Fig. 8, In TEM, a hot-cathode electron gun is heated and produces electrons at high voltage. These electrons are accelerated and form a beam with a certain amount of energy. The electron beam passes through condenser lenses and is concentrated into a narrow beam. When the electron beam hits the sample, some electrons will be absorbed or scattered by the sample, and some electrons will pass through the sample to form transmission electrons. The transmitted electrons pass through the objective lens (which forms the actual microscopic image) and the projector lens (which magnifies the microscopic image) and are then projected onto a fluorescent screen or electronic sensor to form the image.

TEM also has its disadvantages. Due to the easy scattering and absorption of electrons, the penetration of the electron beam emitted by the electron gun is low, and the density and thickness of the sample will affect the final image quality, so ultra-thin slices must be used for observation, usually with a thickness of 50 to 100 nm.

In the study of superconducting materials, TEM can provide high-resolution images at the atomic level, allowing researchers to directly observe the crystal structure of superconducting materials. For example, Fig. 9a depicts the image of $BaPb_{1-x}Bi_xO_3$ material under TEM. This is essential for understanding the microscopic mechanisms of superconductivity, such as coordination and lattice distortion. It can provide detailed information about the microstructure and physical properties of superconducting materials, which will help researchers to deeply understand the nature of superconducting phenomena and guide the design and optimization of superconducting materials.

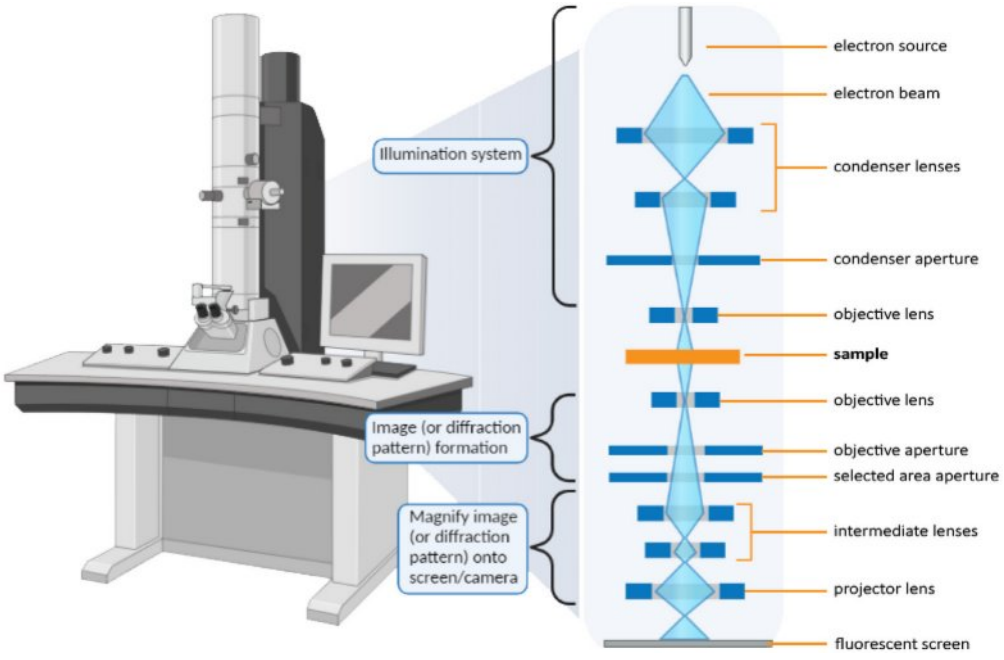

Fig. 8. Simplified TEM diagram [23].

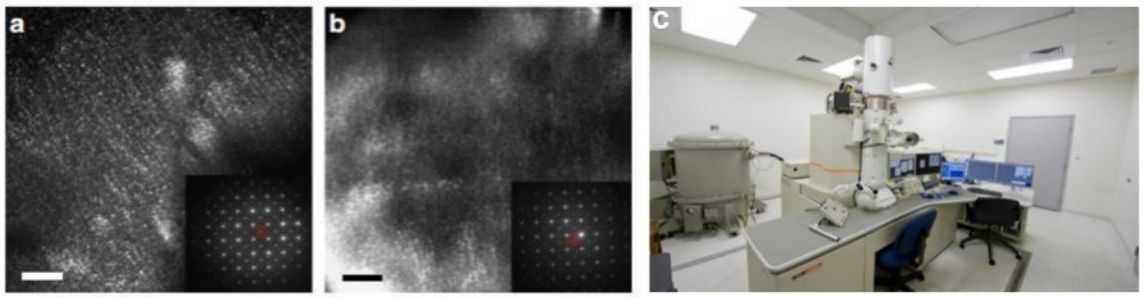

Fig. 9. (a-b) Dark field transmission electron microscopy images for $BaPb_{1-x}Bi_xO_3$ [13], (c) Transmission electron microscopy [25].

Powder-in Tube

Powder tube installation (PIT) is a common method for preparing superconducting wire strips. At present, there are many companies capable of mass production of kilometer-long belts, such as: Beijing INNOST Company (INNOST), Japan's SUMITOMO Electric Company (SUMITOMO), American Superconductor Company (AMSC), Germany's BRUKER Company (BRUKER) and many other companies.

The main principle of this method is that the required various materials are made into powder, mixed together in a certain proportion of metering forms, and loaded into the prepared metal sleeve. After that, it is made into a wire by spinning, drawing, rolling and other processes. Finally, the superconducting wire is formed by heat treatment and sintering. The schematic shown in Fig. 10 illustrates the principle of PIT. For heat treatment methods, in 2006, Sumitomo Electric Corporation of Japan established a 30 MPa cold wall Controlled Overpressure (CT-OP) heat treatment scheme to prepare strips with a critical current of up to 150A, which has attracted great attention from related industries. In the field of superconductivity research, PIT is widely used to prepare high-temperature superconducting wires, such as Bi-2223 ($Bi_2Sr_2Ca_2Cu_3O_{10+x}$) and YBCO ($YBa_2Cu_3O_{7-x}$) wires. These wires play an important role in many applications, including magnets, power transmission lines, electric motors, and generators.

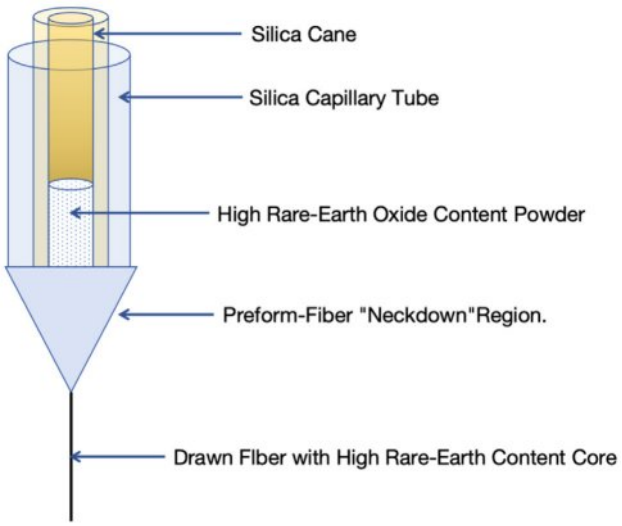

Fig. 10. Powder-in Tube method.

Physical Property Measurement System (PPMS)

Resistivity is an important physical quantity to characterize the resistance characteristics of materials, which is only determined by the substance itself, and is related to the magnetic field, pressure, temperature, and other factors in the environment where the substance is located. Resistivity is the resistance of a particular substance measured at room temperature multiplied by its cross-sectional area divided by its length. In the environment with little temperature change, for standard resistors, the resistivity of the metal is basically linear with the temperature. But for superconducting materials, when the temperature drops to a very low, specific temperature, the resistivity plummets close to zero.

Integrated Physical Property Measurement System (PPMS) has full automatic magnetic, electrical, thermal topography, and other physical property measurement capabilities. Using PPMS, it is possible to measure many material properties such as AC-DC resistivity, differential resistance, thermal conductivity, thermoelectric effect,

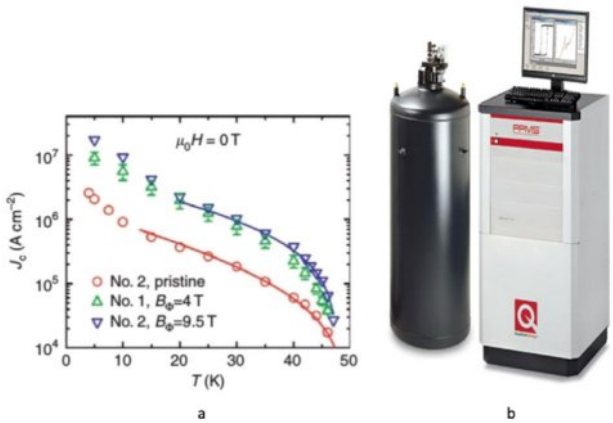

Fig. 11. (a) For $SmFeAsO_{0.8}F_{0.15}$, J_c as a function of temperature for the pre-irradiated sample no. 1, postirradiated sample no. 1 (B_φ=4 T) and sample no. 2 (B_φ=9.5 T) [26], (b) Physical Property Measurement System [27].

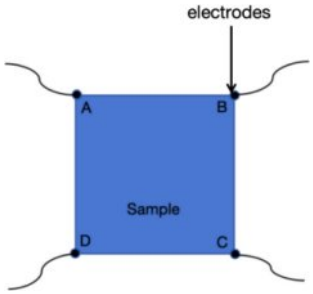

Fig. 12. Vanderbilt method for resistivity measurement.

thermomagnetic curve, Seebeck coefficient, voltammetry characteristics, critical current, magnetoresistance, Hall coefficient, AC susceptibility, specific heat, hysteresis loop, and morphology characterization. In the research field of high-temperature superconducting materials, it is often used to measure the resistivity of materials in different temperature environments. Within a PPMS, there is a basic system that includes a sample chamber, liquid helium dewar, temperature-controlled flow resistance, vacuum pump, superconducting magnet and power supply, electronic control, and data processing systems. In addition, there are extended feature options to help PPMS achieve more physical property measurements. Fig. 11a displays the current density images of $SmFeAsO_{0.8}F_{0.15}$ at different temperatures and magnetic fields using a PPMS.

Taking A Quantum Design PMS-9 as an example, the Vanderbilt method is used to measure the resistivity of the film sample, and four symmetrical electrodes A, B, C, and D are made on the side, as shown in Fig. 12.

When using PPMS to measure the resistivity of the film, the PPMS will, in turn, divide the potential difference between the two electrodes on the side between AB, BC, CD, and DA to obtain the resistance R by the corresponding current. Then we put the value of R into the equation below to find the value of resistivity.

$$\rho = \frac{\pi d}{ln2} \frac{R_{AB,\,CD} + R_{BC,\,DA}}{2} f\left(\frac{R_{AB,\,CD}}{R_{BC,\,DA}}\right) \quad (1)$$

In formula (1), ρ is the resistivity and d is the distance between two adjacent electrodes. Diamagnetism is a kind of basic magnetism of the material, when the material is affected by the external magnetic field, the material will produce a magnetic field in the direction opposite to the external magnetic field, thus resisting the influence of the external magnetic field. This phenomenon is called diamagnetism. Diamagnetism is a universal phenomenon, and all substances exhibit diamagnetism to some degree. In most substances, however, this effect is weak and is often masked by other types of magnetism, such as paramagnetism or ferromagnetism. The principle of diamagnetism is mainly related to the orbital motion and spin motion of electrons. In the absence of an external magnetic field, the movement of electrons in a substance is irregular, and the magnetic fields generated by each electron cancel each other, and the total magnetic properties of the substance are zero. When there is an external magnetic field, the motion orbit of the electron will be changed, resulting in a magnetic field that is opposite to the external magnetic field, which is the source of diamagnetism.

An interesting property of diamagnetic substances is that they are repelled by strong magnetic fields. This is because when the diamagnetic material is placed in the magnetic field, a magnetic field in the opposite direction of the external magnetic field will be generated inside the material so that the material moves from the high magnetic field area to the low magnetic field area, which is reflected in the phenomenon of being repelled by the magnetic field. This property is precisely the key to scientific research and technological applications such as magnetic levitation and superconductivity.

PPMS can also be used to detect and verify the diamagnetism of superconducting materials, known as the Meissner effect. In PPMS, the main method for measuring magnetic susceptibility is the AC magnetic susceptibility technique. Here is the basic principle: The sample is placed in an alternating magnetic field, which causes the sample to magnetize, producing a susceptibility. Magnetic susceptibility is the response of a sample to a change in the magnetic field and can be defined as the ratio of the sample magnetization (M) to the applied magnetic field (H) : χ=M/H. The magnetic susceptibility of diamagnetic substances is less than zero, indicating that they will magnetize in the direction opposite to the external magnetic field. This is because the magnetic moment generated by the orbital motion of the electrons of the diamagnetic material is in the opposite direction of the external magnetic field; The magnetic susceptibility of paramagnetic substances is greater than zero, indicating that they will magnetize in the same direction as the external magnetic field. This is because the spin magnetic moments of the unpaired electrons of a paramagnetic substance align with the external magnetic field; The magnetic susceptibility of ferromagnetic materials is much greater than zero, indicating that they will be strongly magnetized in the external magnetic field. The magnetization of a ferromagnetic substance is due to the cooperative effect of the electron's spin magnetic moment and orbital magnetic moment. In a PPMS system, the magnetization of the sample is measured by an induction coil. When the sample is magnetized, an electromotive force is generated in the induction coil, which is directly related to the magnetization of the sample. Thus, by measuring this electromotive force, we can obtain the magnetization of the sample. In order to improve the accuracy and sensitivity of the measurement, PPMS systems usually use lock-in amplifiers for measurement. The phase-locked amplifier can accurately measure the signal at the same frequency as the reference signal,

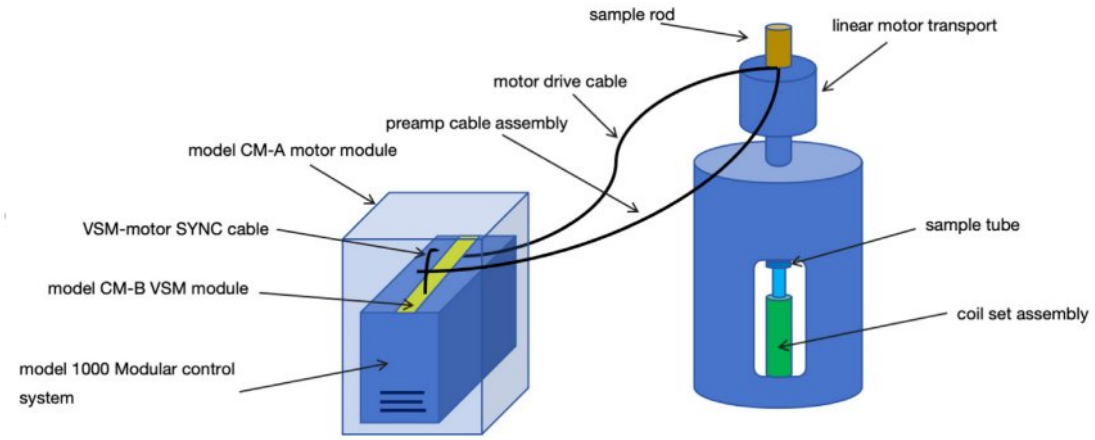

Fig. 13. PPMS structure diagram.

thus eliminating the effect of background noise. By measuring the magnetization of the superconducting sample at different magnetic fields and temperatures, we can get the relationship between the magnetic susceptibility of the sample and the magnetic field and temperature, so as to understand the magnetic properties of the superconducting sample.

The measurement of superconducting transition temperature

The superconducting transition temperature (T_c) of superconducting materials serves as one of the crucial indicators for assessing their performance, holding significant implications for both research and applications. Traditionally, the T_c is often measured using the transport method, which involves determining the change in resistance with temperature. However, due to limitations in experimental conditions, measurement precision, and other factors, traditional methods can introduce certain errors and uncertainties.

To achieve more accurate measurements of T_c in high-temperature superconducting materials, scholars have introduced a novel measurement device. This device leverages low-temperature refrigeration technology and incorporates an advanced temperature control system and data acquisition system, enabling precise temperature control and accurate data collection for samples. Specifically, the device continuously and uniformly cools the sample temperature from room temperature to 35K, simulating the actual working environment of superconducting materials. During this cooling process, the device monitors and records changes in sample resistance, allowing for an accurate determination of T_c.

To eliminate the impact of thermoelectric potential on measurement results, the device employs a current reversal technique. By alternately changing the direction of the current, it cancels out resistance errors caused by the thermoelectric effect, thereby enhancing measurement

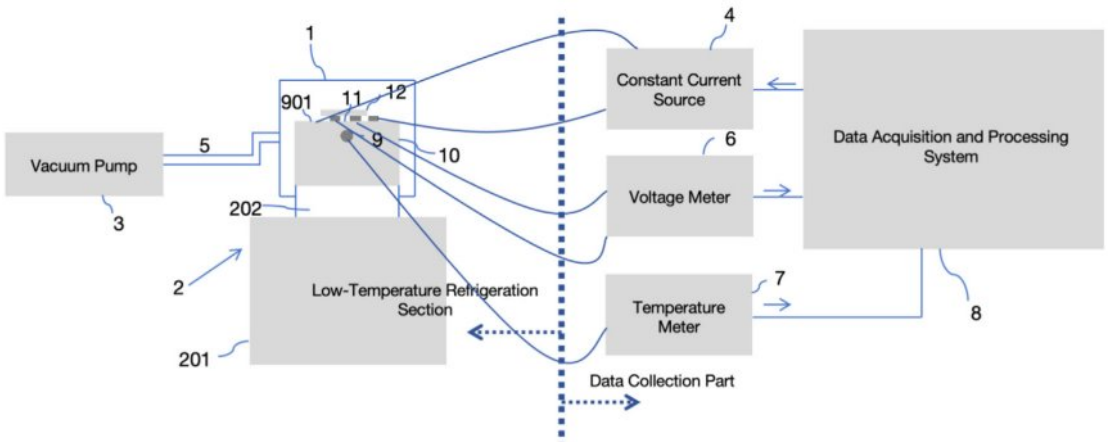

1-Vacuum Cover, 2-Refrigeration Machine, 201-Compressor, 202-Cold Head,3-Vacuum Pump, 5-Vacuum Valve, 9-Thermometer, 901-Sample Lead, 10-Sample Holder, 11-Sample Under Test, 12-Lead Wire

Fig. 14. Schematic Diagram of Low-Temperature Testing System for Superconducting Transition Temperature Measurement.

accuracy. Additionally, for user convenience and data processing, the measurement device integrates a LabVIEW-based data acquisition system with a user-friendly interface. This interface enables users to monitor the experimental process real-time, adjust experimental parameters, and export experimental data for subsequent analysis.

Experimental validation has demonstrated the device's high measurement precision and good reproducibility. Consistent results have been obtained for the same superconducting material across multiple experiments, and compared to traditional methods, the error is significantly reduced. Therefore, this measurement device serves as an effective means for evaluating the performance of high-temperature superconducting materials, providing robust support for both research and applications in this field.

The Development of High-Temperature Superconducting Materials and Several Important High-Temperature Superconducting Materials

In 1986, the breakthrough discovery of high-temperature superconducting materials was made by the German physicist J. G. Bordnorz and the Swiss physicist K. A. Muller, who discovered the T_c=30 K perovskite $La_{2-x}Ba_xCuO_4$ system (lanthanum barium Cupric oxygen system) [28]. Since then, high-temperature superconducting materials have changed from the high-cost liquid helium working environment to the greatly reduced cost of liquid nitrogen working environment, and under the exploration of many scientists, there has been one copper oxide high-temperature superconducting material after another. For example, YBaCuO with 100 K T_c [29], BiSrCaCuO with 110 K T_c [30], TiBaCaCuO with 110 K T_c [31], and HgBaCaCuO with 135 K T_c [32]. The conductivity of copper-based high-temperature superconducting materials has also become a hot topic in condensed matter physics.

Currently, there are several most commonly used systems for high-temperature superconducting materials.

Bi series

The first is the Bi series (BiSrCaCuO). In 1975, Wilmington et al. [33] discovered $BaPb_{1-x}Bi_xO_3$ with T_c of 13 K. This critical superconducting temperature is much higher than that of all previous superconductors without transition elements. In January 1988, Maeda et al. [34] first discovered BiSrCaCuO superconducting material with T_c 105 K. Among them, there are two major systems used in industrial research, namely Bi2223 and Bi2212 systems [35]. The initial main research object was Bi2223, which was prepared using the powder tube loading method (PIT). Its advantage is that its internal structure and superconductivity have strong anisotropy, so the use of heat treatment or mechanical deformation and other methods can get a good texture. However, Bi2223 also has its defects, that is, when it is in the working environment of liquid nitrogen, its (irreversible magnetic field is very low, with the increase of the magnetic field, its critical current density will be rapidly reduced, and because it must use metal silver, high material cost, cost performance is difficult to improve and other factors, so that it is basically eliminated by the market). Therefore, the research direction gradually turns to Bi2212 [12], which is prepared by the metal precursor method. The advantage of Bi2212 is that its superconductivity at liquid helium temperature and strong magnetic field is better than that of low-temperature superconductivity and Bi2223. In order to achieve easier device processing, multi-core and twisted cable, it can be processed into isotropic circular lines by drawing.

Of course, in order to improve the superconducting properties of Bi2212, scientists have tried many methods, and the first three came to mind: doping with electrostatic carriers [36], high pressure [37], and controlling the size of the superconductor at the atomic level [38]. Of these, high pressure is the most promising. This method is based on the theory that Bi_2Te_3, Sb_2Se_3, H_2S and WTe214-16 all become superconductors under certain pressures. So how do you get high pressure? Recently, Tiansheng Liu, Chao He, Fengying Wang et al. realized that a large amount of heat and gas generated by explosions can generate high temperature and high pressure in the form of shock waves [39]. They used

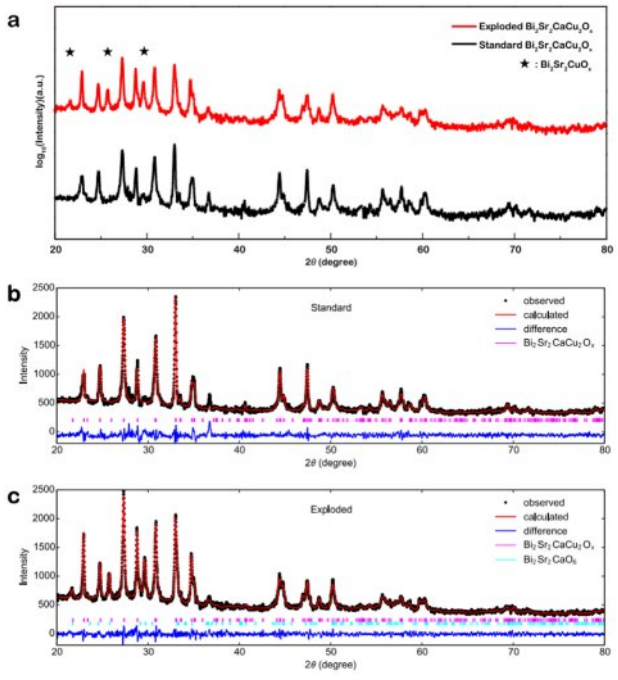

Fig. 15. XRD comparison between the original and shock wave-treated Bi2212. (a) Original sample (black) and processed sample (red line) XRD pattern, the asterisk indicates the newly generated phase. Rietveld refinement results corresponding to the original sample (b) and the treated sample (c).

XRD, TEM, SQUID and other experimental instruments to observe the structure after the explosion.

As shown in Fig. 15, The black dot is the experimental data, the red curve is the fitting result, the blue curve represents the difference between the experiment and the fitting result, and the short vertical line is the predicted position of the diffraction peak. By comparing the XRD patterns of the original and shock-wave treated samples, in addition to the original Bi2212 phase, there is also a newly generated Bi2201 phase, and it can be determined that the superconducting phases Bi2212 and Bi2201 are present in the sample after the explosion. In addition, the superconducting transition temperature of Bi2212 increased from 84 K to 94 K.

However, Bi2212 also has its defects, that is, its low current density in the operating environment in the liquid nitrogen temperature zone, precursor powder and heat treatment process requirements are high, precious metal silver sheath caused by impurity phase, cavity, weak connection, and low-cost performance problems.

4.2 MgB_2, MoB_2 superconductor

In 2001, Jun Nagamatsu et al. [40] processed magnesium (Mg, 99.9%) and processed into powdered amorphous boron (B, 99%) were dried and mixed at a ratio of 1:2 to obtain the sample. The samples were treated at high argon pressure for ten hours in a hot isostatic pressing (HIP) furnace. By X-ray diffraction of the powder, it is found that MgB_2 has a transition temperature of 39 K. This discovery was a breakthrough event that set off a major milestone in the development of high-temperature superconducting materials. After this, in order to discover the unique properties of magnesium diboride, under the guidance of BCS theory, scientists have carried out a lot of research and exploration. According to the BCS theory, the superconducting ground state is generated by the exchange of virtual phonons between electrons, and the electrons with opposite momentum and spin near the Fermi plane form a bound electron pair state through attractive interaction, which is called the Cooper pair. The calculation of the electronic structure shows that magnesium diboride has a strong quantum state density and covalent B-B bond, and thus exhibits strong electron-phonon interaction. MgB_2 occurs in the so-called AlB_2 structure. Boron forms a primitive honeycomb lattice consisting of graphite-type sheets stacked without displacement. Boron forms A hexagonal prism with a base diameter of about 3.5 A,

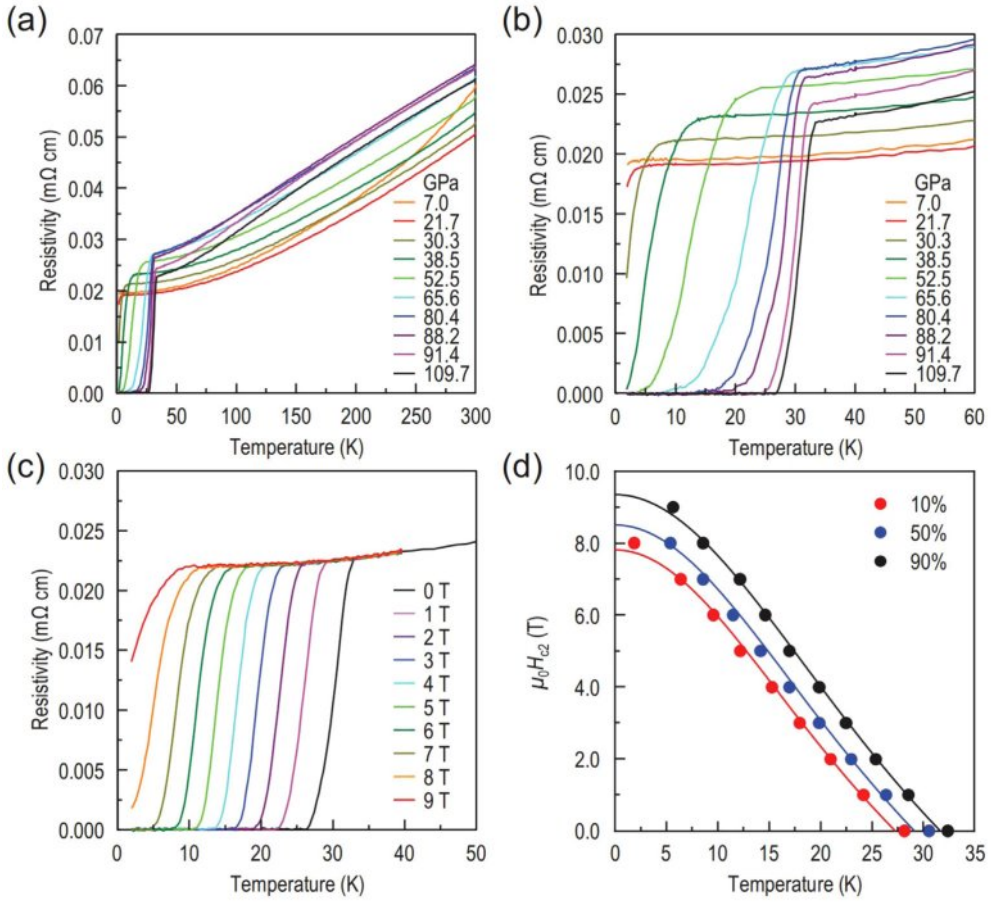

Fig. 16. (a) The variation rule of the electrical resistivity ρ (T) of MoB_2 with temperature under different pressures; (b) superconductive saltation with near amplified ρ (T) curve; (c) The resistivity ρ (T) under different magnetic fields at 109.7 GPa; (d) Temperature dependence of the upper critical field $\mu_0 H_{c2}$ (T) at 109.7 GPa.

equal to the height. This creates nearly spherical pores for Mg. As with graphite, B-B bonds within planes are much shorter than the distances between planes, so B-B bonds are very anisotropic. It is found that boron can effectively enhance the superconducting properties of binary oxides. For example, in Rb-B, Ca-B and La-B systems, boron plays an irreplaceable role. Pressure has always been an important parameter of thermodynamics, and by controlling the pressure of the environment, the properties of materials can be controlled and changed. Recently, Cuiying Pei, Jianfeng Zhang,Qi Wang et al. [41] found that MoB_2 has superconducting properties and a superconducting transition temperature of 32K at 100 GPa. They measured the structural evolution of MoB_2 under different pressures using X-ray diffraction (XRD).

It is found that although both α-MoB_2 and MgB_2 have AlB_2-type structure and certain T_c, the electron-phonon coupling properties of the two compressed superconductors are quite different. In MgB_2 and α-MoB_2, the active phonon mode directly modulates the source electron band, resulting in a strong electron-phonon coupling. However, it is the out-of-plane Mo phonons that directly modulate the d electrons of Mo in α-MoB_2, rather than the stretched B phonon mode that modulates the p bits of B in MgB. It can be guessed that if it contains both magnesium and molybdenum, it will not have a better effect. E. Bayazit, S. Altin, and M.E. Yakinci [42] studied the effects of adding Mo to MgB_2/Ag prepared by the non-in-situ PIT method on its magnetic properties and critical current density Jc properties.

Fig. 17 shows the DC magnetization curve of the sample in relation to temperature. For x = 0.0, that is, pure MgB_2 without Mo, the cell parameters a = 3.0917 Å and c = 3.5298 Å; For x=0.0005s, the peak value of MgB_2 phase decreases and Mo phase appears. Then, with the increase of Mo content, this phenomenon becomes more and more obvious. It is found that Mo atom may not occupy any atomic position in MgB_2 cell. Then, by magnetizing the sample, it was found that Mo concentration significantly affected the onset T_c of MgB_2 tape, and T_c decreased with the increase

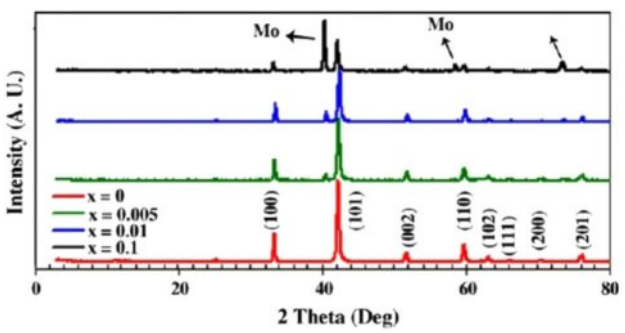

Fig. 17. XRD pattern of Mo added to MgB_2 bandThe XRD patterns of the Mo-added MgB_2 tapes [42].

Table 1. The critical current density J_c at different temperatures at 0T and the critical temperature value T_c of the prepared tape [31].

Addition, x	J_c (Acm^{-2})×10^4			T_c (K)
	10K	20K	30K	
0.0	12.0	8.13	3.89	39.0
0.005	9.79	4.39	1.54	37.5
0.01	9.37	4.07	1.23	36.8
0.1	2.99	0.83	0.81	34.0

Table 2. Logarithmic averages of electron-phonon interactions and phonon frequencies [32].

Phase	Pressure (GPa)	λ	ω_{log}	T_c (K)
MgB_2(P6/mmm)[1]	0	0.80	737	34
MgB_2(P6/mmm)[2]	\	\	\	39
$Mg_{0.333}Mo_{0.667}B_2(R\bar{3}m)$[1]	0	0.62	298	7.4
$Mg_{0.333}Mo_{0.667}B_2(R\bar{3}m)$[1]	25	0.52	373	5.3
$Mg_{0.333}Mo_{0.667}B_2(R\bar{3}m)$[1]	50	0.50	415	5.2
$Mg_{0.5}Mo_{0.5}B_2$(Immm)[1]	0	0.32	460	0.43
$Mg_{0.5}Mo_{0.5}B_2$(Immm)[1]	25	0.36	506	1.12
$Mg_{0.5}Mo_{0.5}B_2$(Immm)[1]	50	0.32	575	0.53

of Mo content. Inspired by this discovery, recently, Prutthipong Tsuppayakorn-aek, Wei Luo et al. [43] began to investigate the compound $Mg_{1-x}Mo_xB_2$ in order to provide basic insights into the structural behavior and electronic properties of the metallic states of $Mg_{1-x}Mo_xB_2$ under different pressures. The ground state structure of $Mg_{1-x}Mo_xB_2$ is revealed by using CE technique and PSO algorithm in the framework of DFT-based evolution. The stability of $Mg_{0.667}Mo_{0.333}B_2$, $Mg_{0.5}Mo_{0.5}B_2$, and $Mg_{0.333}Mo_{0.667}B_2$ against decomposition into MgB_2 and MoB_2 under ambient pressure was confirmed.

The tabular results above highlight the importance of molybdenum substitution in magnesium diboride as it relates to the realization of high T_c superconductors. The results are expected to encourage further experimental studies of these superconducting materials.

Iron-based superconductors

In 2000, the Jeitsch-koteam [44] in Germany synthesized a relatively complete RFeAsO system by adding the powder material with an atomic ratio of R : Fe : FeO : As=3:1:1:3 into 2 g NaCl and KCl with the component ratio of 1:1, and then conducting heat treatment in vacuum treated silica gel tube. In February 2008, the research group of Hosono [45] in Japan found superconductivity of 26 K T_c in LaFeAsO by replacing oxygen atoms with doped F. The material system Hosono's team has discovered can be represented by RFeAsO, a rare earth

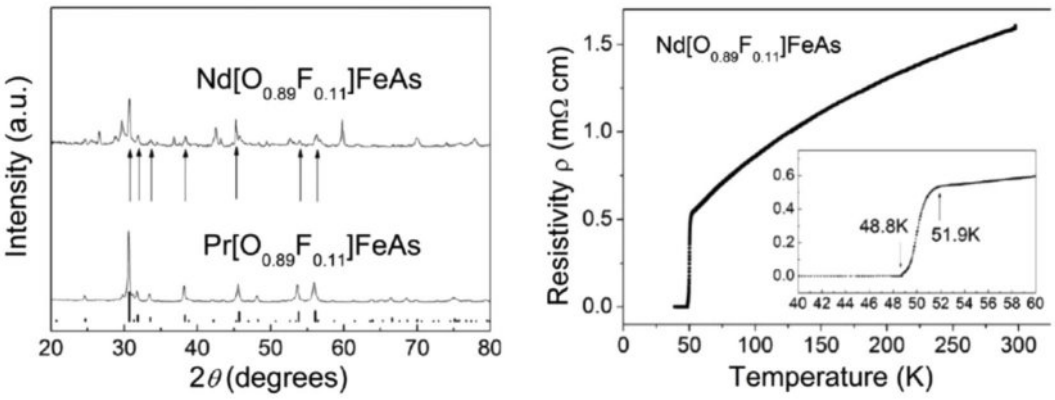

Fig. 18. Comparison of XRD images of (a) $Nd[O_{0.89}F_{0.11}]FeAs$ superconductor and $Pr[O_{0.89}F_{0.11}]FeAs$ superconductor, (b) Temperature-dependent resistivity of $Nd[O_{0.89}F_{0.11}]FeAs$ superconductor [46].

element.

In the same year, the team of Zhao Zhongxian in China, through the experience and equipment of high-pressure synthesis, replaced most of the rare earth elements to the position of lanthanum and observed by XRD technology, and found a large number of superconductors with superconducting transition temperatures exceeding 50 K, such as $Nd[O_{1-x}F_x]FeAs$ [46], and maintained the record of the highest superconducting temperature of 55 K for many years. The analysis of XRD Fig. 18(a) shows that the impurity phase is formed by the initial chemical substance and does not have superconducting properties at the measured temperature. By comparing the XRD images of $Pr[O_{0.89}F_{0.11}]FeAs$, it can be found that the peak of $Nd[O_{0.89}F_{0.11}]FeAs$ is obviously shifted to the right, indicating that the lattice parameter of $Nd[O_{0.89}F_{0.11}]FeAs$ superconductor has decreased lattice constant. As can be clearly seen in Fig. 18(b), when the external temperature drops to 51.9 K, the resistivity drops sharply, and when the temperature is lower than 48.8 K, the resistivity can no longer be measured. Therefore, when the T_c starting point of $Nd[O_{0.89}F_{0.11}]FeAs$ is basically the same as that of $Pr[O_{0.89}F_{0.11}]FeAs$, the temperature of 50.1 K in the middle is higher than that of $Pr[O_{0.89}F_{0.11}]FeAs$ 5 K.

So far, the research on iron-based superconductors has become a hot topic.

In 2009, Wen Haihu's team [47] discovered Sr_2VO_3FeAs with a superconducting transition temperature of 37.2 K employing XRD and measurement of resistivity data in low-temperature regions under different fields. In 2010, Chen Xiaolong et al. [48] of the Chinese Academy of Sciences discovered $K_{1-x}Fe_{2-y}Se_2$ with a superconducting transition temperature of 32K. In the same year, Fang Minghu's team at Zhejiang University [49] discovered $Tl_{1-x}Fe_{2-y}Se_2$ with a superconducting transition temperature of 31K. In 2014, Chen Xianhui et al. made a single layer of iron-selenium superconducting film with a superconducting transition temperature of 50 K, contributing to the operation of iron-based superconductors at temperatures above liquid. In 2014, the team synthesized the layered intercalated superconductor $Li_{1-x}Fe_xOHFeSe$ [50].

Conclusion

In 1911, H.K. Onnes discovered superconductivity in metallic mercury, but the microscopic mechanism was only explained by the BCS theory in 1957. However, in 1986, Bednorz and Müller discovered high-temperature superconducting materials beyond BCS theory, leading to explorations of new theories. Strong correlation electron theory explains electron behavior in complex systems, while spin fluctuation theory attributes high-temperature superconductivity to electron spin fluctuations. These mechanisms are linked to material thermodynamics.High-temperature superconducting materials revolutionized the field, enabling transitions from liquid helium to liquid nitrogen environments.

Researchers continue to develop new oxide materials like YBaCuO, BiSrCaCuO, and HgBaCaCuO. Copper-based superconductivity is a significant area in condensed matter physics.Bismuth-based compounds, especially Bi2212, exhibit superior superconductivity but face limitations like low current densities at liquid nitrogen temperatures. MgB2 and MoB2 superconductors are also crucial. MgB2's discovery marked a milestone, revealing boron's role in enhancing superconducting performance, and pressure as a key thermodynamic parameter. MoB2's superconducting properties were recently discovered, emphasizing molybdenum substitution's importance. Iron-based superconductors are another hot topic. Discoveries of superconductivity in RFeAsO, LaFeAsO, and numerous superconductors with transition temperatures above 50 K have spurred further research. Recent findings include Sr_2VO_3FeAs, $K_{1-x}Fe_{2-y}Se_2$, and $Tl_{1-x}Fe_{2-y}Se_2$, expanding the realm of iron-based superconductors.In conclusion, the future of high-temperature superconducting materials lies in deepening our understanding of Bi series, MgB_2, MoB_2, and iron-based superconductors. Research will focus on

enhancing transition temperatures, optimizing material performance, and reducing costs. Overcoming current challenges promises a bright future for these material.

References

1. S. Łoś, K. Paprocki, K. Fabisiak and M. Szybowicz, Carbon 143(2019) 413-418.
2. K. Joshi, I. Kurtz, Z. Shi, and A.Z. Genack, Nat. Commun. 15[1] (2024) 10616.
3. S.M. So, H.W. Hwang, S.H. Yi, J.S. Park, K.H. Kim, K.H. Lee, J. Park, and S.G. Lee, J. Ceram. Process. Res. 21(2020) S16-S22.
4. G. Grissonnanche, Y. Fang, A. Legros, S. Verret, F. Laliberté, C. Collignon, J. Zhou, D. Graf, P. A. Goddard, L. Taillefer and B. J. Ramshaw, Nature 595[7869] (2021) 667-672.
5. Y.H. Yun, H.W. Han, M.J. Choi, and S.C. Choi, J. Ceram. Process. Res. 6[3] (2005) 259-262.
6. M. Kameneva, L.P. Kozeeva, A.G. Blinov, N. Kuratieva, and V. Fedorov, J. Ceram. Process. Res. 10(2009) 61-65.
7. Y. Liu, T. Wei, G. He, Y. Zhang, Z. Wang, and J. Wang, Nature 618[7967] (2023) 934-939.
8. N. Shimamura, K. Sugawara, S. Sucharitakul, S. Souma, K. Iwaya, K. Nakayama, C.X. Trang, K. Yamauchi, T. Oguchi, K. Kudo, T. Noji, Y. Koike, T. Takahashi, T. Hanaguri, and T. Sato, ACS Nano 12[11] (2018) 10977-10983.
9. M. Nanko, D. Maruoka, H. Ozawa, S. Kamado, H. Abe, A. Kondo, and M. Naito, J. Ceram. Process. Res. 10[6] (2009) 840-843.
10. Q. Jiang, D. Duan, H. Song, Z. Zhang, Z. Huo, S. Jiang, T. Cui, and Y. Yao, Adv. Sci. 11[35] (2024) 2405561.
11. Y. Zhu and X. Yao, Prog. Solid State Chem. 73(2024) 100438.
12. C.B. Cai, Y. Zhao, and Q.G. Uo, Phys. 49[11] (2020) 747-754.
13. P. Kováč, I. Hušek, A. Rosová, M. Kulich, J. Kováč, T. Melišek, L. Kopera, M. Balog, and P. Krížik. Sci. Rep. 8[1] (2018) 11229.
14. M.N. Wilson, Superconducting magnets (1983).
15. J. Bardeen, L.N. Cooper, and J.R. Schrieffer, Phys. Rev. 108[5] (1957) 1175.
16. Nobel Prize, https://www.nobelprize.org/prizes/physics/1972/summary/.
17. P.F. Shan, N.N. Wang, and J.P. Sun, Phys. 50[4] (2021) 217-227.
18. S.L. Li and P.C. Dai, Phys. 40[06] (2011) 353-359.
19. C. Shull and F. Wedgwood, Phys. Rev. Lett. 16 (1966) 513.
20. J. Orenstein and A.J. Millis, Science 288 (2000) 468.
21. X. Xing, C. Wang, L. Yu, J. Xu, C. Zhang, and M. Zhang, Nat. Commun. 14[1] (2023) 5991.
22. LabX, https://www.labx.com/item/bruker-d8-advance-powder-x-ray-diffraction-xrd-system/4262755.
23. Nanoscience, https://www.nanoscience.com/techniques/transmission-electron-microscopy/.
24. P. Giraldo-Gallo, Y. Zhang, C. Parra, H.C. Manoharan, M.R. Beasley, T.H. Geballe, M.J. Kramer, and I.R. Fisher, Nat. Commun. 6[1] (2015) 8231.
25. Nano, http://www.nano.pitt.edu/node/237.
26. L. Fang, Y. Jia, V. Mishra, C. Chaparro, V.K. Vlasko-Vlasov, A. E. Koshelev, U. Welp, G.W. Crabtree, and W.K. Kwok, Nat. Commun. 4[1] (2013) 2655.
27. QD USA, https://www.qdusa.com/products/ppms.html.
28. J.G. Bednorz and K.A. Müller, Z. Phys. B Condens. Matter 64[2] (1986) 189-193.
29. L.C. Bourne, Phys. Lett. A 120 (1987) 494-496.
30. C. Michel, Z. Phys. B Condens. Matter 68[4] (1987) 421-423.
31. Z.Z. Sheng, Phys. Rev. Lett. 60[10] (1988) 937-940.
32. D. Pelloquin, M. Hervieu, C. Michel, G. Van Tendeloo, A. Maignan, and B. Raveau, Physica C: Superconductivity 216[3-4] (1993) 257-263.
33. A.W. Sleight, J.L. Gillson, and P.E. Bierstedt, Solid State Commun. 88[11] (1993) 841-842.
34. H. Maeda, Y. Tanaka, M. Fukutomi, and T. Asano, Jpn. J. Appl. Phys. 27[2A] (1988) L209.
35. W.-H. Yan, C.-B. Cai, and D.-F. Zhou, Phys. 48[11] (2019) 733-748.
36. J.T. Ye, Y. Zhang, R.J. Akashi, M. Bahramy, S. Arita, and Y. Iwasa, Science 338[6111] (2012) 1193-1196.
37. Y. Liu, X. Shen, Q.Q. Liu, X. Li, S.M. Feng, R.C. Yu, S. Uchida, and C.Q. Jin, Physica C: Superconductivity 497 (2014) 34-37.
38. W.H. Zhang, Y. Sun, J.S. Zhang, F.S. Li, M.H. Guo, Y.F. Zhao, H.M. Zhang, J.P. Peng, Y. Xing, and H.C. Wang, Chinese Phys. Lett. 31[1] (2014) 017401.
39. T. Liu, C. He, F. Wang, Y. Liu, X. Xi, R. Zhong, and G. Gu, Sci. Rep. 7[1] (2017) 6710.
40. C.B. Cristina and T.Y. Tsutomu, Supercond. Sci. Technol. 14[11] (2001) R115.
41. M.S. Torikachvili, S.L. Bud'ko, N. Ni, and P.C. Canfield, Phys. Rev. Lett. 101[5] (2008) 057006.
42. E. Bayazit, S. Altin, M.E. Yakinci, M.A. Aksan, and Y.A. Balci, J. Alloys Compd. 457[1-2] (2008) 42-46.
43. P. Tsuppayakorn-Aek, W. Luo, and R. Ahuja, Sci. Rep. 13[1] (2023) 20295.
44. P. Quebe, L.J. Terbüchte, and W. Jeitschko, J. Alloys Compd. 302[1] (2000) 70-74.
45. Y. Kamihara, T. Watanabe, M. Hirano, and H. Hosono, J. Am. Chem. Soc. 130[11] (2008) 3296-3297.
46. Z.A. Ren, J. Yang, W. Lu, W. Yi, X.L. Shen, Z.C. Li, G.C. Che, X.L. Dong, L.L. Sun, and F. Zhou, Europhys. Lett. 82[5] (2008) 57002.
47. X. Zhu, F. Han, G. Mu, P. Cheng, B. Shen, B. Zeng, and H.H. Wen, Phys. Rev. B 79[22] (2009) 220512.
48. J. Guo, S. Jin, G. Wang, S. Wang, K. Zhu, T. Zhou, M. He, and X. Chen, Phys. Rev. B 82[18] (2010) 180520.
49. M.H. Fang, H.D. Wang, C.H. Dong, Z.J. Li, C.M. Feng, J. Chen, and H.Q. Yuan, Europhys. Lett. 94[2] (2011) 27009.
50. X.F. Lu, N.Z. Wang, H. Wu, Y.P. Wu, D. Zhao, X.Z. Zeng, X.G. Luo, T. Wu, W. Bao, G.H. Zhang, F.Q. Huang, Q.Z. Huang, and X.H. Chen, Nat. Mater. 14[3] (2015) 325-329.